ISSN 1990-4789, Journal of Applied and Industrial Mathematics, 2022, Vol. 16, No. 1, pp. 70–79. © Pleiades Publishing, Ltd., 2022.
Russian Text © The Author(s), 2022, published in Sibirskii Zhurnal Industrial'noi Matematiki, 2022, Vol. 25, No. 1, pp. 67–79.

Localization of the Discontinuity Lines of the Bottom Scattering Coefficient According to Acoustic Sounding Data

E. O. Kovalenko[1*] **and I. V. Prokhorov**[1,2**]

[1] *Institute of Applied Mathematics, Far East Branch, Russian Academy of Sciences, Vladivostok, 690041 Russia*

[2] *Far Eastern Federal University, Vladivostok, 690090 Russia*

e-mail: *kovalenkoq@gmail.com, **prokhorov@iam.dvo.ru

Received August 18, 2021; revised November 17, 2021; accepted January 13, 2022

Abstract—The paper considers the mathematical problems of constructing sonar images of the seabed from the data of measurements of a multibeam side-scan sonar. For the nonstationary radiative transfer equation describing the process of acoustic sounding in the ocean, we investigate the inverse problem of finding the discontinuity lines of the bottom scattering coefficient. A numerical algorithm for solving the inverse problem is developed, and the analysis of the quality of localization of the boundaries of inhomogeneities of the seabed depending on the number of angles and the sounding range is carried out.

Keywords: *radiative transfer equation, inverse problem, diffuse reflection condition, bottom and volume scattering, discontinuity line of function, multibeam sounding*

DOI: 10.1134/S1990478922010069

INTRODUCTION

The radiative transfer equation describes a wide variety of physical processes and is used in the design of nuclear reactors, in astrophysics and atmospheric optics, in X-ray and optical tomography, and in gas dynamics and acoustics. We consider the radiative transfer equation in the context of modeling the process of high-frequency acoustic sounding in a fluctuating ocean [1–5]. Our interest in the model is due to the specific goal of improving the quality of sonar images of the seabed according to measurements obtained from a side-scan sonar (SSS) installed on autonomous unmanned underwater vehicles (AUV) [6–9].

The mathematical model includes a monochromatic integro-differential transfer equation, an initial condition, and a boundary condition describing the diffuse reflection from the bottom surface [9–16]. For simplicity, it is assumed that the carrier of the receiving-transmitting antenna emitting a pulsed signal moves at a constant speed in a certain straight line. The inverse problem is to find the bottom scattering coefficient under some additional conditions for redefining the solution of the radiative transfer equation, the physical meaning of which is to measure the backward reflected signal.

For a narrow radiation pattern in the single-scattering approximation, an explicit solution was obtained in [16] to find the diffuse reflection coefficient, the use of which leads to defocusing bottom objects on sonar images as the width of the radiation pattern increases. Attempts to eliminate this defect in single-beam probing are often unsuccessful, because the resulting system of linear algebraic equations has an ill-conditioned matrix when the problem is discretized and the solution of the problem becomes sensitive to errors in the initial data [17]. To overcome the difficulties that arise, one resorts to the use of multibeam echo sounders or to an increase in the number of tacks when monitoring water areas [7, 8]. The papers [18, 19] propose an approximate method for finding the bottom scattering coefficient from multibeam sounding data, which, despite its efficiency, has

a number of significant drawbacks and requires additional a priori information about the acoustic characteristics of the medium.

In the present paper, we suggest to modify the statement of the original problem assuming that the desired characteristic is not the reflection coefficient but only the lines where the coefficient undergoes a discontinuity of the first kind. Information about the discontinuity lines of the coefficient is often sufficient to determine the location and shape of the desired object. The interest in inverse problems in which it is required to find the discontinuity surfaces or the singular support of a function is quite high and is connected, first of all, with integral geometry problems [21–25]. Generalized statements of such problems were considered in [26, 27] and consisted in determining the discontinuity surfaces of the coefficients of the stationary radiative transfer equation from information about the radiation emerging from the medium.

In practice, the number of angles of sounding the medium is relatively low, and we are dealing with the so-called problems of few-view tomography [28]. The main part of the known results in this area deals with the problem of inverting the Radon transform based on incomplete data. More complex problems concerning the partial localization of the discontinuity surfaces of the coefficients of the stationary radiative transfer equation for one- and two-angle probing were considered in the relatively recent papers [29–32].

1. DIRECT AND INVERSE PROBLEMS FOR NONSTATIONARY RADIATIVE TRANSFER EQUATION

The mathematical model under consideration describing the propagation of high-frequency acoustic wave fields in scattering media is based on a nonstationary radiative transfer equation of the form [6–19]

$$\left(\frac{1}{c}\frac{\partial}{\partial t} + \mathbf{k}\cdot\nabla_r + \mu\right) I(\mathbf{r},\mathbf{k},t) = \frac{\sigma}{4\pi}\int\limits_{\Omega} I(\mathbf{r},\mathbf{k}',t)\,d\mathbf{k}' + J(\mathbf{r},\mathbf{k},t), \tag{1}$$

where $\mathbf{r}\in G\subset\mathbb{R}^3$, $t\in[0,T]$, and the wave vector $\mathbf{k}$ belongs to the unit sphere $\Omega=\{\mathbf{k}\in\mathbb{R}^3 \mid |\mathbf{k}|=1\}$. The function $I(\mathbf{r},\mathbf{k},t)$ is interpreted as the energy flux density of a wave propagating in the direction $\mathbf{k}$ with velocity c at time t at point $\mathbf{r}$. The numbers μ and σ have the meaning of attenuation and scattering coefficients, and the function J describes the sound field sources.

The domain G is the upper half-space bounded by the horizontal plane $\gamma=\{\mathbf{r}=(r_1,r_2,r_3)\in\mathbb{R}^3 \mid r_3=-l\}$, $l>0$. Equation (1) is supplemented with the initial and boundary conditions [13, 14]

$$I^-(\mathbf{r},\mathbf{k},t)|_{t<0}=0, \quad (\mathbf{r},\mathbf{k})\in G\times\Omega, \tag{2}$$

$$I^-(\mathbf{y},\mathbf{k},t) = \frac{\sigma_d(\mathbf{y})}{\pi}\int\limits_{\Omega_+} |\mathbf{n}\cdot\mathbf{k}'| I^+(\mathbf{y},\mathbf{k}',t)(\mathbf{y},\mathbf{k}',t)\,d\mathbf{k}, \quad (\mathbf{y},\mathbf{k},t)\in\Gamma^-. \tag{3}$$

In relations (2), (3), we use the notation

$$I^\pm(\mathbf{y},\mathbf{k},t) = \lim_{\varepsilon\to-0} I(\mathbf{y}\pm\varepsilon\mathbf{k},\mathbf{k},t\pm\varepsilon/c),$$
$$\Gamma^\pm = \big\{(\mathbf{y},\mathbf{k},t)\in\gamma\times\Omega_\pm\times(0,T)\big\},$$
$$\Omega_\pm = \big\{\mathbf{k}\in\Omega \mid \operatorname{sgn}(\mathbf{n}\cdot\mathbf{k})=\pm1\big\},$$

where $\mathbf{n}=(0,0,-1)$ is the unit outward normal vector on the boundary of the domain G. Condition (2) means that there is no radiation in the medium at the initial time, and the boundary condition (3) describes the effects of diffuse reflection from the seabed by the Lambert law with reflection coefficient $\sigma_d(\mathbf{y})$. The function $\sigma_d(\mathbf{y})$ varying on the interval from zero to one in the γ-plane is also called the bottom scattering coefficient. It is assumed that the γ-plane on which the function $\sigma_d(\mathbf{y})$ is defined can be represented as the union of disjoint two-dimensional subdomains γ_i, $i=0,\dots,p$, with piecewise smooth boundaries $\partial\gamma_i$ such that $\sigma_d(\mathbf{y})$ is constant in each of the domains γ_i.

Problem 1. Equation (1) with the initial and boundary conditions (2), (3) and with given μ, σ, σ_d, J, and c forms an initial–boundary value problem of finding the unknown function I on the set $G \times \Omega \times (0, T)$.

The papers [13–19] deal with the well-posedness of Problem 1, also known as the direct problem for the radiative transfer equation.

The function J, which describes a point pulsed sound source moving at a constant velocity V in the positive direction of the r_2-axis, has the form

$$J(\mathbf{r}, \mathbf{k}, t) = \delta(\mathbf{r} - \mathbf{V}t) \sum_{i=1}^{m} \delta(t - t_i), \quad \mathbf{V} = (0, V, 0), \quad t_i > 0, \tag{4}$$

where δ is the Dirac delta function. Let us supplement the system of relations (1)–(3) with the relation

$$\int_{\Omega} S_j(\mathbf{k}) I^+(\mathbf{V}t, \mathbf{k}, t)\, d\mathbf{k} = P_j(t), \quad j = 1, \ldots, q, \tag{5}$$

where the function $S_j(\mathbf{k})$ is integrable, nonnegative, and distinct from zero only in some subdomain $\Omega_j \subset \Omega$. We state the following inverse problems.

Problem 2. Find the function $\sigma_d(\mathbf{y})$ from relations (1), (2), (3), (5) for given μ, σ, c, V, J, l and S_j, and $P_j(t)$.

Problem 3. Find the lines of discontinuity $\partial\gamma_i$, $i = 0, \ldots, p$, of the function $\sigma_d(\mathbf{y})$ from relations (1)–(3), (5) for given V, J and S_j, and $P_j(t)$.

As was already mentioned, the physical meaning of the inverse Problem 2 is to reconstruct the reflection coefficient σ_d during acoustic sounding of the seabed by a side-scan sonar that moves rectilinearly at a constant velocity V and sounds the surrounding space with pulsed signals. There are antennas on the carrier that measure the total intensity $P_j(t)$ in the field of view Ω_j at time t, and the functions $S_j(\mathbf{k})$ characterize the radiation pattern of the jth antenna. If $q = 2$, $\Omega_1 = \{\mathbf{k} \in \Omega \mid k_1 < 0\}$, and $\Omega_2 = \{\mathbf{k} \in \Omega \mid k_1 > 0\}$, then we are dealing with the simplest case of a side-scan sonar with one receiving antenna on each side of the carrier [9].

Problem 3 is to determine not the function σ_d itself but only its discontinuity lines $\partial\gamma_i$ with much less information about the initial data of the problem. In particular, the quantities μ and σ are not supposed to be known, but they cannot be determined in such a statement of the problem either. Problem 2 was studied in [18, 19], and so the main attention will be focused on Problem 3. As applied to X-ray tomography problems, similar problems for the stationary transport equation were considered in [26, 27, 29–32]. These papers propose original methods based on constructing an inhomogeneity indicator, which permit efficiently reconstructing the discontinuity surfaces of the coefficients of the radiative transfer equation. Note that in Problem 3 we determine the lines of discontinuity of the coefficient $\sigma_d(\mathbf{y})$, which occurs in the boundary condition (3) rather than in Eq. (1).

2. EXPRESSIONS FOR THE FUNCTIONS $P_j(t)$ IN THE SINGLE-SCATTERING APPROXIMATION

As a rule, the antenna carrier velocity V, the medium parameters μ, σ, and c, and the sounding periods $t_{i+1} - t_i$ are such that $(\sigma/\mu)^2 \ll 1$, $V/c \ll 1$, and $\exp(-\mu c|t - t_i|) \ll 1$, $t \notin (t_i, t_{i+1})$. This gives grounds to apply the single-scattering approximation to find a solution of the initial–boundary value problem and to neglect echolocation signals from the other sounding periods (t_j, t_{j+1}), $j \neq i$, at the current reception interval $t \in (t_i, t_{i+1})$ [10].

Under the above-indicated conditions, the approximate solution of the initial–boundary value problem (1)–(3) has the form [18, 19]

$$I(\mathbf{r}, \mathbf{k}, t) = I_0(\mathbf{r}, \mathbf{k}, t) + I_\gamma(\mathbf{r}, \mathbf{k}, t) + I_G(\mathbf{r}, \mathbf{k}, t), \tag{6}$$

where

$$I_0(\mathbf{r},\mathbf{k},t)=\int\limits_0^{d(\mathbf{r},-\mathbf{k},t)}\exp(-\mu\tau)J(\mathbf{r}-\tau\mathbf{k},\mathbf{k},t-\tau/c)\,d\tau, \tag{7}$$

$$\begin{aligned}I_\gamma(\mathbf{r},\mathbf{k},t)=\frac{\sigma_d\big(\mathbf{r}-d(\mathbf{r},-\mathbf{k},t)\mathbf{k}\big)}{\pi}\exp\big(-\mu d(\mathbf{r},-\mathbf{k},t)\big)\\ \times\int\limits_{\Omega_+}|\mathbf{n}\cdot\mathbf{k}'|I_0^+\left(\mathbf{r}-d(\mathbf{r},-\mathbf{k},t)\mathbf{k},\mathbf{k}',t-\frac{d(\mathbf{r},-\mathbf{k},t)}{c}\right)d\mathbf{k}',\end{aligned} \tag{8}$$

$$I_G(\mathbf{r},\mathbf{k},t)=\int\limits_0^{d(\mathbf{r},-\mathbf{k},t)}\exp(-\mu\tau)\frac{\sigma}{4\pi}\int\limits_\Omega I_0\left(\mathbf{r}-\tau\mathbf{k},\mathbf{k}',t-\frac{\tau}{c}\right)d\mathbf{k}'d\tau. \tag{9}$$

In the expressions (7)–(9), we use the notation $d(\mathbf{r},-\mathbf{k},t)=\min\{d(\mathbf{r},-\mathbf{k}),ct\}$, where $d(\mathbf{r},-\mathbf{k})$ is the distance from a point $\mathbf{r}\in G$ in the direction $-\mathbf{k}$ to the boundary of the domain G. If $\mathbf{r}-d(\mathbf{r},-\mathbf{k},t)\mathbf{k}\notin\partial G$, then $I_\gamma=0$. The simple structure of the domain G allows one to write an explicit representation $d(\mathbf{r},-\mathbf{k},t)=\min\{l/k_3,ct\}$ of the function $d(\mathbf{r},-\mathbf{k},t)$ at the points belonging to the plane $r_3=0$ for $k_3>0$ and $d(\mathbf{r},-\mathbf{k},t)=ct$ for $k_3\le 0$. By substituting I_0, $I\gamma$, and I_G into (5), we obtain

$$P_j(t)=P_{j,0}(t)+P_{j,\gamma}(t)+P_{j,G}(t), \tag{10}$$

where

$$P_{j,0}(t)=\int\limits_\Omega S_j(\mathbf{k})I_0^+(\mathbf{V}t,\mathbf{k},t)\,d\mathbf{k}, \tag{11}$$

$$P_{j,\gamma}(t)=\int\limits_\Omega S_j(\mathbf{k})I_\gamma^+(\mathbf{V}t,\mathbf{k},t)\,d\mathbf{k}, \tag{12}$$

$$P_{j,G}(t)=\int\limits_\Omega S_j(\mathbf{k})I_G^+(\mathbf{V}t,\mathbf{k},t)\,d\mathbf{k}. \tag{13}$$

Taking into account the structure of the function J and the paper [18], we obtain

$$P_{j,0}(t)=0,$$

$$P_{j,\gamma}(t)=\frac{cl^2}{2\pi}\frac{\exp\big(-\mu c(t-t_i)\big)}{\big(c(t-t_i)/2\big)^5}\int\limits_0^{2\pi}S_j\big(\mathbf{k}(\varphi,\theta_i)\big)\sigma_d\big(\mathbf{y}(\varphi,\theta_i)\big)\,d\varphi, \tag{14}$$

$$P_{j,G}(t)=\frac{\sigma c\exp\big(-\mu c(t-t_i)\big)}{8\pi\big(c(t-t_i)/2\big)^2}\int\limits_0^{2\pi}\int\limits_{\theta_i}^{\pi}S_j\big(\mathbf{k}(\theta,\varphi)\big)\sin\theta\,d\theta d\varphi, \tag{15}$$

where $\mathbf{k}(\theta,\varphi)=(-\sin\varphi\sin\theta,\cos\varphi\sin\theta,\cos\theta)$, the angle θ varies from $\theta_i=\arccos\left(\dfrac{2l}{c(t-t_i)}\right)$ to π, and $\varphi\in[0,2\pi)$.

If the receiving antenna pattern S_j is narrowly directed in planes perpendicular to the bottom surface $r_3=-l$,

$$S_j\big(\mathbf{k}(\theta,\varphi)\big)=\delta(\varphi-\varphi_j),$$

where $\delta(\varphi-\varphi_j)$ is the Dirac delta function, then formulas (14) and (15) for $t\in(t_i+2l/c,t_{i+1})$ acquire the very simple form

$$P_{j,\gamma}(t)=\frac{cl^2c}{2\pi}\frac{\exp\big(-\mu c(t-t_i)\big)}{\big(c(t-t_i)/2\big)^5}\sigma_d\big(\mathbf{y}(\varphi_j,\theta_i)\big), \tag{16}$$

$$P_{j,G}(t) = \frac{\sigma c \exp\big(-\mu c(t-t_i)\big)}{8\pi\big(c(t-t_i)/2\big)^2}\left(1+\frac{2l}{c(t-t_i)}\right). \tag{17}$$

In this case, for determining the function σ_d, from (10), (14), and (15) for any j we obtain the explicit formula [18]

$$\sigma_{d,j}(\mathbf{y}) = \left(P_j\left(t\right) - \frac{\sigma c \exp\big(-2\mu|\mathbf{y}-\mathbf{V}t|\big)}{8\pi|\mathbf{y}-\mathbf{V}t|^2}\left(1+\frac{l}{|\mathbf{y}-\mathbf{V}t|}\right)\right)\left(\frac{cl^2}{2\pi}\frac{\exp\big(-2\mu|\mathbf{y}-\mathbf{V}t|\big)}{|\mathbf{y}-\mathbf{V}t|^5}\right)^{-1}, \tag{18}$$

where $t = (y_2 + y_1\cot\varphi_j)/V$. Thus, for a narrowly collimated (in the angle φ) radiation pattern, formula (18) gives an explicit solution of Problem 2 in the single-scattering approximation. Obviously, in this case it suffices to carry out measurements using two receiving antennas located on different sides of the carrier, say, with $S_1 = \delta(\varphi - \pi/2)$ and $S_2 = \delta(\varphi - 3\pi/2)$; this corresponds to the widespread method of constructing sonar images successively strip by strip perpendicular to the direction of motion of the antenna carrier.

With an increase in the width of the radiation pattern, the calculation of the function σ_d by formula (18) leads to an increase in the error, especially when reconstructing high-contrast structures. On sonar images, the so-called effect of "smearing," or defocusing, of the image appears. To eliminate such defects, various focusing methods are used, which in mathematical terms are reduced to solving an integral equation of the first kind. When the desired function is discretized, the solution of the integral equation is equivalent to the solution of an (as a rule, ill-conditioned) system of linear algebraic equations; this considerably complicates determining the desired function [17].

Another, in our opinion, the most important drawback of the algorithm for reconstructing the bottom scattering coefficient by using formula (18) is due to the fact that additional information about the attenuation and volume-scattering coefficients is required. As a rule, the coefficients of Eq. (1) that describe the interaction of radiation in the ocean are known only approximately; therefore, the reconstruction of the bottom scattering coefficient by formula (18) leads to large distortions of tomographic images.

Thus, the construction of numerical algorithms for solving Problem 3 that require much less information about the initial data and are free from most of the indicated drawbacks is really important for the development of modern methods of acoustic sounding of the seabed.

3. NUMERICAL ALGORITHM FOR SOLVING INVERSE PROBLEM 3

In this section, we present a numerical scheme for solving the inverse Problem 3. As we have already noted, the problem under consideration can be viewed as a problem of few-view tomography, and the algorithm for solving it is close to the methods described in the papers [29–32].

Let the radiation pattern $S_j(\mathbf{k}(\varphi,\theta))$ be equal to

$$S_j(\mathbf{k}(\varphi,\theta)) = \begin{cases} 1/2\beta, & \varphi \in (\varphi_j-\beta, \varphi_j+\beta) \\ 0, & \varphi \notin (\varphi_j-\beta, \varphi_j+\beta), \end{cases}$$

with the support of each of the functions S_j concentrated either in the interval $0 < \pi/2 - \delta/2 < \varphi < \pi/2 + \delta/2$ or in the interval $0 < 3\pi/2 - \delta/2 < \varphi < 3\pi/2 + \delta/2$, where $\delta < \pi$. The latter restriction is typical of scanning the seabed with a side-scan sonar and makes it possible to recover the function σ_d separately for $r_1 > 0$ and $r_1 < 0$ [8–10]. When constructing the algorithm and carrying out numerical experiments, we consider only the half-plane $r_3 = -l$, $r_1 > 0$, and the value of the exponent q corresponds not to the total number of sounding angles but only to one of the "shipboards" of antenna carrier motion.

Taking into account the stated constraints and the relation

$$|\mathbf{V}t - \mathbf{y}|^2 = y_1^2/\sin^2\varphi_j + l^2 \quad \text{for} \quad t = (y_2 + y_1\cot\varphi_j)/V,$$

the expressions for the functions $P_{j,\gamma}((y_2+y_1\cot\varphi_j)/V)$ and $P_{j,G}((y_2+y_1\cot\varphi_j)/V)$ can be written in the form

$$\begin{aligned}
&P_{j,\gamma}\big((y_2+y_1\cot\varphi_j)/V\big)\\
&\quad=\frac{c\,l^2c}{2\pi}\frac{\exp\left(-2\mu\sqrt{y_1^2/\sin^2\varphi_j+l^2}\right)}{(y_1^2/\sin^2\varphi_j+l^2)^{5/2}}\\
&\qquad\times\frac{1}{2\beta}\int\limits_{\varphi_j-\beta}^{\varphi_j+\beta}\sigma_d\big(|y_1|\sin\varphi/|\sin\varphi_j|,y_2+y_1\cot\varphi_j-|y_1|\cos\varphi/|\sin\varphi_j|\big)\,d\varphi\\
&\quad=\frac{cl^2c}{2\pi}\frac{\exp\left(-2\mu\sqrt{y_1^2/\sin^2\varphi_j+l^2}\right)}{(y_1^2/\sin^2\varphi_j+l^2)^{5/2}}\\
&\qquad\times\frac{1}{2\beta}\int\limits_{\varphi_j-\beta}^{\varphi_j+\beta}\sigma_d\big(|y_1|\sin\varphi/|\sin\varphi_j|,y_2+|y_1|(\cos\varphi_j-\cos\varphi)/|\sin\varphi_j|\big)\,d\varphi,
\end{aligned}\tag{19}$$

$$\begin{aligned}
&P_{j,G}\big((y_2+y_1\cot\varphi_j)/V\big)\\
&\quad=\frac{c\sigma}{8\pi}\frac{\exp\left(-2\mu\sqrt{y_1^2/\sin^2\varphi_j+l^2}\right)}{(y_1^2/\sin^2\varphi_j+l^2)}\left(1+\frac{l}{\sqrt{y_1^2/\sin^2\varphi_j+l^2}}\right).
\end{aligned}\tag{20}$$

Set

$$\begin{aligned}
\widehat{P}_{j,\gamma}(\mathbf{y})&\equiv P_{j,\gamma}\big((y_2+y_1\cot\varphi_j)/V\big),\\
\widehat{P}_{j,G}(\mathbf{y})&\equiv P_{j,G}\big((y_2+y_1\cot\varphi_j)/V\big),
\end{aligned}$$

where $\mathbf{y}=(y_1,y_2,-l)$ and the functions $P_{j,\gamma}$ and $P_{j,G}$ are defined in (19) and (20). An approximate method for solving the inverse Problem 3 is based on preliminary calculation of functions of the form

$$\widehat{\sigma}_{d,j}(\mathbf{y})=\Big|\nabla\big(\widehat{P}_j(\mathbf{y})A_j(\mathbf{y})\big)\cdot\mathbf{k}_j\Big|\tag{21}$$

for each $\mathbf{k}_j=(\cos\varphi_j,\sin\varphi_j,0)$ and subsequent construction of the indicator function

$$\widehat{\sigma}_d(\mathbf{y})=\sum_{j=1}^{q}\widehat{\sigma}_{d,j}(\mathbf{y}).\tag{22}$$

In Eq. (21), the function $A_j(\mathbf{y})$ is some continuously differentiable weight function selected so as to compensate for a strong decay of the function P as $|y_1|\to\infty$. For example, if we know the quantities μ and l or at least their approximate values, then for the function $A_j(\mathbf{y})$ we can take an expression of the form

$$\left(\frac{\exp(-2\mu\sqrt{y_1^2/\sin^2\varphi_j+l^2})}{(y_1^2/\sin^2\varphi_j+l^2)^{5/2}}\right)^{-1}.$$

If, however, there is no a priori information, then we can set $A=1$. One can readily see that the functions $\nabla\widehat{P}_{j,G}(\mathbf{y})\cdot\mathbf{k}_j$ are bounded on the entire range of their arguments, and the

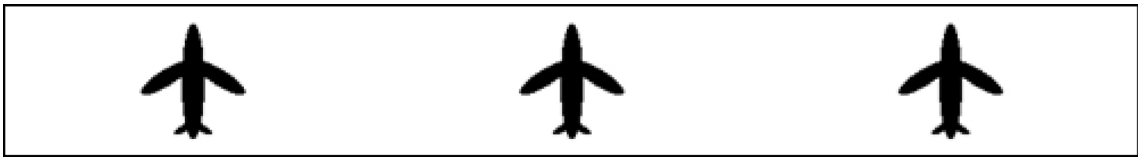

Fig. 1. Graphical representation of the bottom scattering coefficient $\sigma_d(\mathbf{y})$ (original). The linear dimensions of the surveyed bottom area are 300×50 m.

functions $\nabla \widehat{P}_{j,\gamma}(\mathbf{y}) \cdot \mathbf{k}_j$ may grow unboundedly only for the case in which for $\varphi \in [\varphi_j, -\beta, \varphi_j + \beta]$ the line of integration in (19),

$$\begin{aligned} z_1 &= |y_1| \sin\varphi / |\sin\varphi_j|, \\ z_2 &= y_2 + |y_1|(\cos\varphi_j - \cos\varphi)/|\sin\varphi_j|, \\ z_3 &= -l, \end{aligned} \tag{23}$$

intersects the line of discontinuity of the function $\sigma_d(\mathbf{y})$, $\mathbf{y} = (y_1, y_2, -l)$. As the point $\mathbf{y}$ tends to the line of discontinuity $\partial\gamma_i$, the number of terms $\widehat{\sigma}_{d,j}(\mathbf{y})$ in the sum (22) with the indicated property will grow; this leads to the growth of the function $\widehat{\sigma}_d(\mathbf{y})$. The degree of growth of the functions $\widehat{\sigma}_{d,j}(\mathbf{y})$ depends on the angle between the curve (23) and the line of discontinuity at the point of their intersection, and the growth is maximal if the angle is zero, i.e., the curves touch each other. A rigorous substantiation of these facts is hampered by the restriction associated with the discreteness of the set of sounding directions; moreover, it is rather cumbersome and goes beyond the scope of this article. In the next section, we give a numerical confirmation of the efficiency of the algorithm based on the construction of the indicator function (22).

4. RESULTS OF NUMERICAL SIMULATION

When monitoring water areas by autonomous unmanned underwater vehicles, the speed of the carrier, the height of its trajectory above the bottom of the reservoir, and the sounding interval usually depend on the mission objectives, the size of the basin under study, and the features of the equipment. In numerical experiments, the following values of sounding parameters were chosen: $V = 1$ m/s, $l = 12$ m, $t_{i+1} - t_i = 0.4$ s. The receiving antenna beam width in the horizontal plane was 2 deg ($\beta = 1/\pi$), which is typical for most modern side-scan sonars [7, 8]. The remaining quantities took the following values, typical for acoustic sounding in the oceanic medium at frequencies of the order of 100 kHz [5, 9, 11]: $\mu = 0.018$ m^{-1}, $\sigma = 0.1\mu$, $c = 1500$ m/s.

The algorithm for solving the inverse problem was tested for the function $\sigma_d(r)$ whose graphical representation for $r_1 > 0$ is given in Fig. 1. The function σ_d takes the value 0.9 in all three inclusions γ_i, $i = 1, 2, 3$. The domains G_i, $i = 1, 2, 3$, which are inclusions of the "aircraft wreckage" type, are located at distances of 50, 150, and 250 m from the axis $r_1 = 0$, respectively. In the complement $\gamma_0 = \gamma \setminus (\gamma_1 \cup \gamma_2 \cup \gamma_3)$, the function σ_d takes the value 0.1.

Figure 2 shows the images of the functions $\widehat{\sigma}_{d,j}(\mathbf{y})$ calculated using formulas (21) for single-beam probing at the angles $\varphi_1 = \pi/6$, $\varphi_3 = \pi/2$, and $\varphi_5 = 5\pi/6$. The quality of the images corresponding to the angles $\varphi_1 = \pi/6$ and $\varphi_5 = 5\pi/6$ is much lower; this is not surprising, because the sounding range at oblique angles increases. This leads to a deterioration in the resolution of the seabed image reconstruction algorithm.

Figure 3 shows graphic representations of the function $\widehat{\sigma}_d(\mathbf{y})$ for various values of the parameter q. It can be seen from Fig. 3a that the first inclusion is clearly reconstructed only for $q = 5$; therefore, when localizing the lines of discontinuity of the bottom scattering coefficient at a distance of up to 100 m, it suffices to use a small number of sounding angles.

As expected, the quality of object focusing increases with the increase in the number of probing angles. Improving the quality of the tomographic image with an increase in q is especially noticeable at a probing distance of more than 100 m. However, for a high-quality reconstruction of the discontinuity lines of the desired coefficient at a distance of approximately 250 m, an increase in

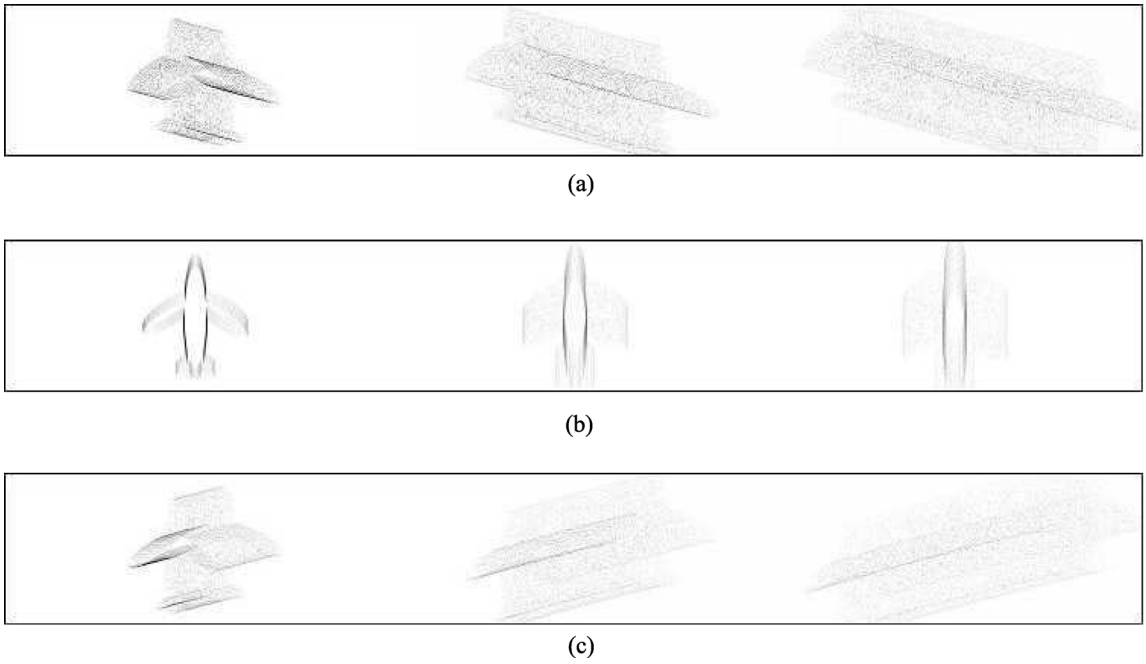

Fig. 2. Reconstructed functions $\widehat{\sigma}_{d,j}(\mathbf{y})$ for $j = 1, 3, 5$ for single-beam sounding with beam width of 2 deg: (a) $\varphi_1 = \pi/6$, (b) $\varphi_1 = \pi/2$, (c) $\varphi_1 = 5\pi/6$.

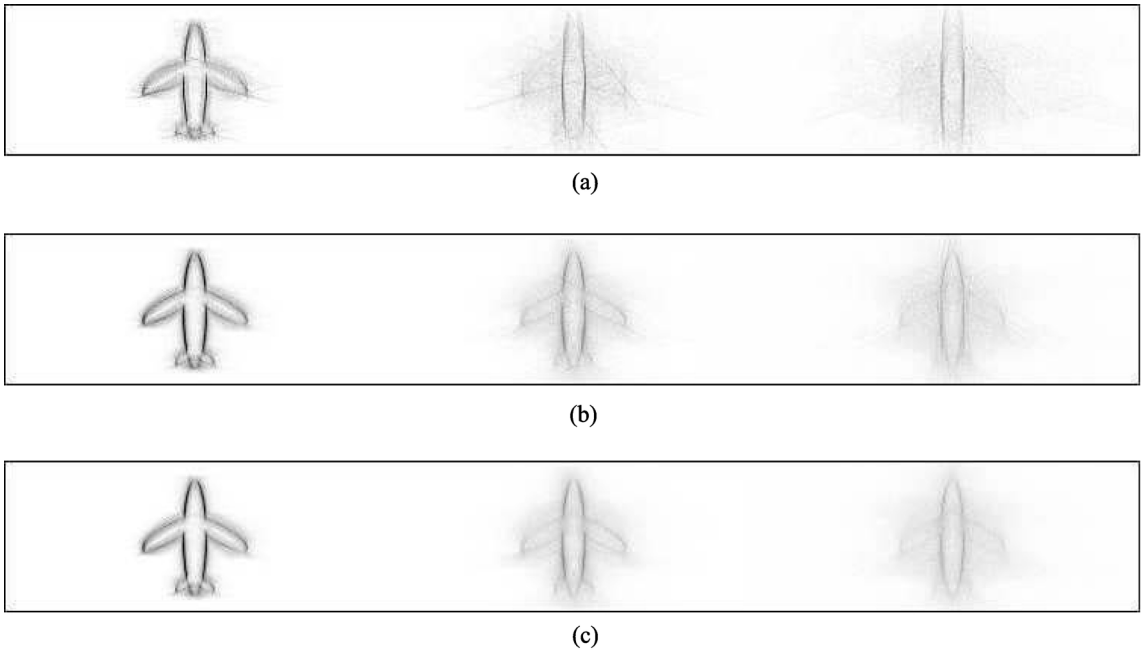

Fig. 3. Function $\widehat{\sigma}_d(\mathbf{y})$ characterizing the set of points of discontinuity of $\sigma_d(\mathbf{y})$ for various numbers q of sounding angles: (a) $q = 5$, (b) $q = 15$, (c) $q = 25$.

the number of angles alone is not sufficient. This is due to an increase in the relative error of the approximate calculation of the function $P_j((y_2 + y_1 \cot \varphi_j)/V)$ with an increase in $|y_1|$.

Note that the deterioration in the seabed image reconstruction quality is also observed with distance from the transmitting-receiving antenna in real physical experiments when monitoring water areas. With an increase in the probing range, a considerable decrease in the useful reflected signal occurs, while the destructive noise in the detection devices remains at the same level. The nature of such noise can be very diverse and associated, say, with a strong instability of the trajectory

of motion of an autonomous unmanned underwater vehicle or with refraction of sound rays due to a change in the density of the marine environment [6–8]. In the most simplified case, a timed automatic gain control algorithm is used to amplify the reflected signal in accordance with the time of its arrival. Despite the fact that today there are already many varieties of such algorithms, it is not possible to completely compensate for the loss in the image reconstruction quality [6–8].

CONCLUSIONS

The inverse problem of finding the discontinuity lines of the bottom scattering coefficient for the nonstationary radiative transfer equation describing the process of acoustic sounding in the ocean is studied. A numerical algorithm for solving the inverse problem has been developed and verified on model data corresponding to acoustic sounding of the seabed at frequencies of the order of 100 kHz. It is shown that for successful localization of discontinuity lines of the bottom scattering coefficient at a distance of up to 100 m, a small number of angles (of the order of 5) is sufficient. With an increase in the sounding range, it is necessary not only to increase the number of sounding angles but also to reduce the error in calculating the functions P_j. In practice, such restrictions impose strict requirements on the transceiver equipment of side-scan sonars.

FUNDING

This work was financially supported by the Russian Foundation for Basic Research, project no. 20-01-00173, and the Russian Ministry of Education and Science, projects nos. 075-01095-20-00 and 075-02-2020-1482-1.

REFERENCES

1. A. Ishimaru, *Wave Propagation and Scattering in Random Media* (Academic Press, New York, 1978).
2. J. A. Turner and R. L. Weaver, "Radiative transfer of ultrasound," J. Acoust. Soc. Am. **96** (6), 3654–3674 (1994).
3. V. I. Mendus and G. A. Postnov, "On the angular distribution of high-frequency dynamic ocean noise," Akoust. Zh. **39** (6), 1107–1116 (1993).
4. G. Bal, "Kinetics of scalar wave fields in random media," Wave Motion **43**, 132–157 (2005).
5. J. E. Quijano and L. M. Zurk, "Radiative transfer theory applied to ocean bottom modeling," J. Acoust. Soc. Am. **126** (4), 1711–1723 (2009).
6. A. V. Bogorodskii, G. V. Yakovlev, E. A. Kopenin, and A. K. Dolzhikov, *Hydroacoustic Technology for Ocean Exploration and Development* (Gidrometeoizdat, Leningrad, 1984) [in Russian].
7. G. Griffiths, *Technology and Applications of Autonomous Underwater Vehicles* (CRC Press, London, 2002).
8. Yu. V. Matvienko, V. A. Voronin, S. P. Tarasov, A. V. Sknarya, and E. V. Tutynin, "Ways to improve hydroacoustic technologies for surveying the seabed using autonomous uninhabited underwater vehicles," Podvodnye Issled. Robototekh. **8** (2), 4–15 (2009).
9. I. V. Prokhorov, V. V. Zolotarev, and I. B. Agafonov, "The problem of acoustic sounding in a fluctuating ocean," Dal'nevost. Mat. Zh. **11** (1), 76–87 (2011).
10. I. V. Prokhorov and A. A. Sushchenko, "Studying the problem of acoustic sounding of the seabed using methods of radiative transfer theory," Acoust. Phys. **61** (3), 368–375 (2015).
11. I. V. Prokhorov, A. A. Sushchenko, and A. Kim, "Initial boundary value problem for the radiative transfer equation with diffusion matching conditions," J. Appl. Ind. Math. **11** (1), 115–124 (2017).
12. I. V. Prokhorov and A. A. Sushchenko, "The Cauchy problem for the radiative transfer equation in an unbounded medium," Dal'nevost. Mat. Zh. **18** (1), 101–111 (2018).
13. A. A. Amosov, "Initial–boundary value problem for the non-stationary radiative transfer equation with diffuse reflection and refraction conditions," J. Math. Sci. **235** (2), 117–137 (2018).

14. I. V. Prokhorov, "The Cauchy problem for the radiation transfer equation with Fresnel and Lambert matching conditions," Math. Notes **105** (1), 80–90 (2019).

15. A. Kim and I. V. Prokhorov, "Initial–boundary value problem for a radiative transfer equation with generalized matching conditions," Sib. Electron. Math. Rep. **16**, 1036–1056 (2019).

16. E. O. Kovalenko, A. A. Sushchenko, and I. V. Prokhorov, "Processing of the information from side-scan sonar," Proc. SPIE **10035**, article ID 100352C (2016).

17. E. O. Kovalenko, A. A. Sushchenko, and V. A. Kan, "Focusing of sonar images as an inverse problem for radiative transfer equation," Proc. SPIE **10833**, article ID 108336D (2018).

18. E. O. Kovalenko and I. V. Prokhorov, "Determination of the coefficient of bottom scattering during multibeam sounding of the ocean," Dal'nevost. Mat. Zh. **19** (2), 206–222 (2019).

19. E. O. Kovalenko, I. V. Prokhorov, A. A. Sushchenko, and V. A. Kan, "Problem of multibeam remote sensing of sea bottom," Proc. SPIE **11208**, article ID 112085P (2019).

20. E. Yu. Derevtsov, S. V. Mal'tseva, and I. E. Svetov, "Determination of discontinuities of a function in a domain with refraction from its attenuated ray transform," J. Appl. Ind. Math. **12** (4), 619–641 (2018).

21. S. V. Mal'tseva, I. E. Svetov, and A. P. Polyakova, "Reconstruction of a function and its singular support in a cylinder by tomographic data," Eurasian J. Math. Comput. Appl. **8** (2), 86–97 (2020).

22. A. Faridani, E. L. Ritman, and K. T. Smith, "Local tomography," SIAM J. Appl. Math. **52** (2), 459–484 (1992).

23. A. Faridani, D. V. Finch, E. L. Ritman, and K. T. Smith, "Local tomography. II," SIAM J. Appl. Math. **57** (4), 1095–1127 (1997).

24. E. T. Quinto, "Singularities of the X-ray transform and limited data tomography in R^2 and R^3," SIAM J. Math. Anal. **24**, 1215–1225 (1993).

25. E. T. Ramm and A. I. Katsevich, *The Radon Transform and Local Tomography* (CRC Press, Boca Raton, 1996).

26. D. S. Anikonov, A. E. Kovtanyuk, and I. V. Prokhorov, *Transport Equation and Tomography* (VSP, Boston–Utrecht, 2002).

27. D. S. Anikonov, V. G. Nazarov, and I. V. Prokhorov, *Poorly Visible Media in X-Ray Tomography* (VSP, Boston–Utrecht, 2002).

28. O. V. Filonin, *Few-View Tomography* (Izd. SNTs Ross. Akad. Nauk, Samara, 2006) [in Russian].

29. D. S. Anikonov, V. G. Nazarov, and I. V. Prokhorov, "The problem of single-beam probing of an unknown medium," J. Appl. Ind. Math. **5** (4), 500–505 (2011).

30. D. S. Anikonov, V. G. Nazarov, and I. V. Prokhorov, "Algorithm of finding a body projection within an absorbing and scattering medium," J. Inverse Ill-Posed Probl. **18** (8), 885–893 (2011).

31. D. S. Anikonov and V. G. Nazarov, "Problem of two-beam tomography," Comput. Math. Math. Phys. **52** (3), 315–320 (2012).

32. D. S. Anikonov, V. G. Nazarov, and I. V. Prokhorov, "An integrodifferential indicator for the problem of single beam tomography," J. Appl. Ind. Math. **8** (3), 301–306 (2014).